

**INVESTIGATION ON THE PROPULSIVE EFFICIENCY OF  
THE SMALL UAV CONCEPTUAL DESIGN**

by

**KHAIRUL IKHSAN YAHAYA**

Thesis submitted in fulfillment of the requirements  
for the Degree of  
Master of Science

(March 2012)

## **ACKNOWLEDGEMENTS**

This work was supported by Universiti Sains Malaysia under award 1001/PAERO/814042. The allowance provided by Institute of Postgraduate Studies through Graduate Assistant (GA) Teaching Scheme is also gratefully appreciated.

I would like to thank my supervisor at Universiti Sains Malaysia, Dr. Kamarul Arifin Ahmad. His technical insight has been invaluable and the flexibility and enthusiasm with which he approaches graduate research and his students has enabled a wonderful environment for growth, professionally and personally.

I would also like to thank Mohammed Zubair of Universiti Sains Malaysia for his technical advice in preparing manuscript and A. R. Serakawi for his technical advice in conducting CFD simulation.

## TABLE OF CONTENTS

Acknowledgement	ii
Table of Contents	iii
List of Tables	vi
List of Figures	vi
List of Symbols	viii
Abstrak	xi
Abstract	xii

### CHAPTER 1 – INTRODUCTION

1.1 Research Background	1
1.2 Problem Statement	2
1.3 Objective	3
1.4 Scope of Work	4
1.5 Thesis Organisation	4

### CHAPTER 2 – LITERATURE REVIEW

2.1 Introduction	5
2.2 Computational Fluid Dynamic (CFD)	7
2.3 Electric engine	7
2.4 Autonomous Subsystem Architecture	9
2.5 Multidisciplinary Optimization (MDO)	11
2.6 Overview on ABL Turbulence and Goldstein Vortex Theory	12
2.7 Summary	13

## **CHAPTER 3 – METHODOLOGY**

3.1	Initial Aerodynamic Characteristic of Small UAV	14
3.1.1	Weight Buildup	15
3.1.2	Critical Performance Parameters	16
3.1.3	Configuration Layout of Small UAV	18
3.2	Computational Fluid Dynamics (CFD) Analyses	20
3.3	Preliminary Performance Analyses	23
3.4	Parametric Study of Propulsive Efficiency	24
3.4.1	BLDC Motor Characteristic	24
3.4.2	The Characteristic of Propeller	26
3.4.3	The Governing Equations of Goldstein’s Vortex Theory	27
3.4.4	Matlab Algorithm	30

## **CHAPTER 4 – RESULTS AND DISCUSSION**

4.1	Small UAV Configuration Layout	33
4.1.1	Total Weight	33
4.1.2	Configuration Layout	33
4.2	Validation of Turbulence Model	36
4.2.1	Mesh Dependency Check	36
4.2.2	Comparison with Existing Experimental Work	38
4.3	Observation of Static Stability and Preliminary Performance Parameter	43
4.4	Parametric Study of Propulsive Efficiency	45
4.4.1	Effect of Airspeed	45
4.4.2	Effect of Propeller Size	47
4.4.3	Effect of Propeller Geometry	49
4.4.4	Effect of BLDC Motor Rated Power	51
4.4.5	The Feasible Propeller-BLDC Motor Combination	53

**CHAPTER 5 – CONCLUSION**

5.1 Conclusion	58
5.2 Future Work Recommendations	59

<b>REFERENCES</b>	<b>60</b>
-------------------	-----------

**APPENDIX A**

**APPENDIX B**

## LIST OF TABLES

		Page
Table 3.1	Performance data of UAV in the market [91]	14
Table 3.2	Sums of $W_{\text{auto-sub}}$ , $W_{\text{payload}}$ and $W_{\text{battery}}$	15
Table 3.3	BLDC motor candidates	25
Table 4.1	Size, planform and arrangement of wing, pylon and empennage	36
Table 4.2	Sizing of control surfaces	36

## LIST OF FIGURES

		Page
Figure 2.1	Schematic of testing rig for fault-tolerant 250 kW Permanent Magnet (PM) power generation system [47]	8
Figure 3.1	The flow chart of CFD simulation procedure	20
Figure 3.2	The flow domain divided into main and smaller region.	21
Figure 3.3	Small UAV computational domain	22
Figure 3.4	Flow chart of function <i>bladetable</i>	32
Figure 4.1(a)	Front view of small UAV	34
Figure 4.1(b)	Side view of small UAV	35
Figure 4.2	Lift slope for mesh dependency check	37
Figure 4.3	Drag polar for mesh dependency check	37
Figure 4.4	The experimental results by Roberts et al [14] for unswept wing; (a)lift in turbulent intensity 1.2%, and (b)lift in turbulent intensity 7.4%	38
Figure 4.5	Lift slope of small UAV compared with experimental results [14]	39
Figure 4.6	ABL turbulence drag polar compared with experimental results [14]	40
Figure 4.7	The experimental results by Roberts et al [14] for unswept wing; (a)drag in turbulent intensity 1.2%, and (b)drag in turbulent intensity 7.4%	41

Figure 4.8	Drag polar at different Re number	42
Figure 4.9	The experimental results of minimum drag at low Re number by Hirata et al [30]	42
Figure 4.10	$C_L^{3/2}/C_D$ ratio against $C_L$ at cruise speed and climb speed	44
Figure 4.11	Constraint diagram of the small UAV	44
Figure 4.12(a)	The thrust coefficient distribution on propeller at different advance ratio at pitch-to-diameter ratio 0.5.	46
Figure 4.12(b)	The torque coefficient distribution on propeller at different advance ratio at pitch-to-diameter ratio 0.5.	46
Figure 4.13(a)	The required torque on propeller variant maximum blade chord ratio 0.075	48
Figure 4.13(b)	The rotational speed of propeller variant maximum blade chord ratio 0.075	48
Figure 4.14(a)	The required torque on propeller at climb condition	50
Figure 4.14(b)	The rotational speed of propeller at climb condition	51
Figure 4.15	Torque/speed characteristic of every BLDC motor [94]	52
Figure 4.16(a)	Propeller rotational speed at maximum speed normalized for Himax HC3516-1130	54
Figure 4.16(b)	Propeller torque at maximum speed normalized for Himax HC3516-1130	54
Figure 4.16(c)	Propeller rotational speed at climb condition normalized for Himax HC3516-1130	55
Figure 4.16(d)	Propeller torque at climb condition normalized for Himax HC3516-1130	56
Figure 4.16(e)	Propeller maximum blade chord ratio 0.05 torque and rotational speed at maximum speed normalized for Himax HA2825-2700	57
Figure 4.16(f)	Propeller maximum blade chord ratio 0.05 torque and rotational speed at climb condition normalized for Himax HA2825-2700	57
Figure B.1	Matrix Ftq0507NH2825	
Figure B.2	Matrix FeasibleFtq0507NH2825	

## LIST OF SYMBOLS

		Unit
$W$	Total weight	kg
$W_{crew}$	Crew weight	kg
$W_{payload}$	Payload weight	kg
$W_{fuel}$	Fuel weight	kg
$W_{empty}$	Empty weight	kg
$W_{auto-sub}$	Weight of autonomous subsystem	kg
$W_{battery}$	Weight of battery	kg
$A, B$	Coefficient of empty weight to total weight logarithmic relation	
$f_{lb-kg}$	Unit conversion factor; lb to kg	
$C_L$	Lift coefficient	
$C_{Lmax}$	3D wing maximum lift coefficient	
$C_D$	Drag coefficient	
$C_{DU_1}$	Drag coefficient at flight condition 1	
$C_{DU_2}$	Drag coefficient at flight condition 2	
$c_{lmax}$	2D airfoil maximum lift coefficient	
$\rho$	Air density	kg/m <sup>3</sup>
$\rho_{100m}$	Air density at altitude 100m	kg/m <sup>3</sup>
$U$	Airspeed	m/s
$U_1$	Airspeed at flight condition 1	m/s
$U_2$	Airspeed at flight condition 2	m/s
$U_{stall}$	Stall speed	m/s
$\frac{W}{S}$	Wing loading	N/m <sup>2</sup>

$\frac{W}{P}$	Power loading	N/W
$\frac{P}{W}$	Power to weight ratio	W/N
$C_{m0}$	Zero lift pitching moment coefficient	
$C_{m\alpha}$	Pitching moment derivative due to angle of attack	
$C_{n\beta}$	Yawing moment derivative due to sideslip force	
$RCP$	Rate of climb parameter	m/s
$RC_0$	Rate of climb at sea level	m/s
$h$	Altitude	m
$h_{abs}$	Absolute altitude	m
$t_{cl}$	Time to climb	s
$P$	Power	W
$\eta$	Propulsive efficiency	
$T$	Thrust	N
$l$	Torque	Nm
$I$	Current	A
$V$	Voltage	V
$\omega$	Rotational speed	rad/s
$\omega_{max}$	Maximum effective rotational speed	rad/s
$K_v$	Back EMF constant	rad/s/V
$K_t$	Torque constant	Nm/A
$R_m$	BLDC motor internal resistance	$\Omega$
$c_b$	Local propeller blade chord	m
$c_{bmax}$	Maximum propeller blade chord	m
$\hat{c}_b$	Local propeller blade chord length ratio	
$d_p$	Propeller diameter	m

$\zeta$	Ratio of local propeller blade chord line radius to propeller radius	
$\zeta_h$	Ratio of propeller hub radius to propeller radius	
$r$	Propeller local radius	m
$\tilde{C}_L$	Lift coefficient of propeller blade chord	
$\tilde{C}_D$	Drag coefficient of propeller blade chord	
$C_T$	Propeller thrust coefficient	
$C_l$	Propeller torque coefficient	
$k$	Number of propeller blade	
$\alpha_b$	Angle of attack of propeller blade chord	rad
$\alpha_{L0}$	Propeller blade zero lift angle of attack	deg
$\beta$	Aerodynamic pitch angle	rad
$\beta_t$	Aerodynamic pitch angle at the blade tip	rad
$\varepsilon_i$	Induced angle	rad
$\varepsilon_\infty$	Advance angle	rad
$K$	Local pitch-to diameter ratio	
$J$	Advance ratio	
$\lambda$	Aerodynamic pitch length	m
$\lambda_c$	Chord line pitch length	m

# **SIASATAN KE ATAS KECEKAPAN DORONGAN DALAM REKABENTUK KONSEP UAV KECIL**

## **ABSTRAK**

Satu kajian berparameter rekabentuk konsep Pesawat Autonomus Tanpa Pemandu(UAV) kecil berketinggian rendah telah dilakukan. Tujuannya untuk menganggarkan kecekapan dorongan dalam gambarajah kekangan oleh sistem dorongan kipas-motor Arus Terus Tanpa Berus (BLDC) pada dua kondisi penerbangan berbeza dengan kesan gelora Lapisan Terbatas Atmosfera (ABL). Cerun daya angkat dan pola daya seret telah diperolehi melalui simulasi kerangka pesawat dalam Fluent<sup>TM</sup> 6.3 menggunakan model gelora SST  $k-\omega$  pada kelajuan pegun, sederhana dan maksimum. Gambarajah kekangan dibina dan beban kuasa pada kondisi penerbangan berbeza diselesaikan sebagai daya dorongan yang diperlukan pada kelajuan udara berbeza. Teori vorteks kipas Goldstein digunakan untuk memodelkan kipas; geometri bilah kipas dan saiz kipas telah divariasikan untuk melihat kesan daya kilas kipas dan kelajuan putaran untuk menghasilkan daya dorongan yang diperlukan apabila dipadankan dengan motor BLDC. Hasil simulasi CFD menunjukkan peningkatan bercorak logaritma dalam daya seretan minimum dengan penurunan kelajuan udara. Tanpa mengambil kira nilai kecekapan dorongan, beban kuasa di titik rekabentuk, ditentukan oleh keperluan kelajuan maksimum adalah kira-kira 0.23 N/W. Himax HA2825-2700 dengan nilai kuasa yang kedua tertinggi, 400 W didapati sebagai motor BLDC yang paling sesuai. Kesimpulan telah dibuat bahawa untuk membina gambar rajah kekangan, nilai kecekapan dorongan oleh kombinasi kipas-motor BLDC terbaik ialah 52 peratus pada keperluan kelajuan maksimum dan 42 peratus pada keperluan mendaki.

# INVESTIGATION ON THE PROPULSIVE EFFICIENCY OF THE SMALL UAV CONCEPTUAL DESIGN

## ABSTRACT

A parametric study of low altitude small Unmanned Autonomous Vehicle (UAV) conceptual design was performed. The purpose was to estimate constraint diagram propulsive efficiency of propeller-Brushless Direct Current (BLDC) motor propulsion system at two different flight conditions with the consideration of Atmospheric Boundary Layer (ABL) turbulent effect. The lift slope and drag polar of the small UAV was obtained by simulating the airframe in Fluent<sup>TM</sup> 6.3 using SST  $k-\omega$  turbulence model at stall, cruise and maximum speeds. Constraint diagram was constructed and power loading at different flight conditions was resolved as required thrust at different airspeed. Goldstein vortex theory of propellers was used to model propeller; the propeller blade geometry and size was varied to see the effect of propeller torque and rotational speed at required thrust and airspeed with BLDC motor matching. CFD simulation results show a logarithmic trend increase in minimum drag with the decrease of airspeed. Without considering the propulsive efficiency of the propulsion system, the power loading at design point, determined by maximum speed requirement was about 0.23N/W. Himax HA2825-2700 with second highest rated power of 400W was found to be the most suitable BLDC motor. It was concluded that for constructing constraint diagram, the propulsive efficiency value of the best BLDC motor-propeller combination was 58 percent for maximum speed requirement and 42 percent for time to climb requirement.

# Chapter 1

## Introduction

### 1.1 Research Background

Aircraft conceptual design is a process of integrating limited initial design information. Wright brothers did a great job integrating information from predecessor gliders in building the Wright Flyer [1]. But being the first to attempt for a powered flight, the information of relationship between engine rated power and flight stability were lacking, thus the Wright Flyer were unfeasible in term of stability [2]. Conceptual design methodology of small Unmanned Autonomous Vehicle (UAV) is the same as conceptual design methodology of manned aircraft, except that the factor of unmanned, and autonomous control need to be added into design consideration. As accepted by US Army [3], any UAV with total weight between 0.907 to 4.54 kg can be considered as small UAV. For consistency, unless mentioned in the original literature, all UAVs within that range of total weight are regarded as small UAV.

The minimum required power of propulsion system is an important parameter during the conceptual design stage of any small UAV, like in the case of any other aircraft. Constraint diagram or matching plot is a popular method for determining this parameter [4-7]. For a propeller driven aircraft this parameter is characterized by takeoff power loading  $(W/P)_{TO}$  for a given wing loading  $(W/S)$ . This method assists the aircraft designers to get an early insight on the requirement of the minimum rated power to perform some of the most demanding task/flight condition in the aircraft's entire mission profile.

Raymer [8] and Roskam [9,10] provided standard guidelines for optimizing the wing loading  $(W/S)$  and take-off power loading  $(W/P)_{TO}$  by selecting appropriate wing configuration and propulsion system. The brushless DC (BLDC) motor combined with propeller is a popular

mean of propulsion in small UAVs. Unlike fueled reciprocating engines that depend on purely mechanical operation to drive a propeller, a BLDC motor converts the electrical energy into mechanical operation which then drives the propeller. Lundström et al [11] has carried out experiments to validate BLDC motor propulsive efficiency and efficiency of speed controller provided by manufacturers. Gur and Rosen [12] investigated the interactions between various components of BLDC propulsion system and concluded that battery density and maximum power-to-mass ratio have the biggest influence on the design and performance of BLDC propulsion system. Meanwhile Ragot et al [13] developed a method that optimized BLDC motor configuration. This configuration is a compromise between maximum efficiency and minimum weight.

## **1.2 Problem Statement**

Most previous literature [11-13] did not investigate the propulsive efficiency at different flight conditions. At different flight conditions, small UAVs often operate at different airspeed and the propeller would also operate at different advance ratio. The propulsive efficiency of propulsion system with propeller depends on the operating advance ratio. Without appropriate value of propulsive efficiency aircraft designer could not tell whether the rated electrical power of propulsion system could provide the required mechanical power at any flight condition. For a propeller driven aircraft, the required mechanical power on propeller is different at different flight condition. To counter aerodynamic the drag at different airspeed the propeller also generates thrust at different rotational speed.

In the experimental work by Lundström et al [11], propellers by different manufacturers were tested and the readings of current were averaged. Different manufacturer normally do not produce their propeller with identical geometry. Ignoring the effect of propeller geometry could have contributed an error in averaging the readings of current. The study by Gur and Rosen [12] is more toward developing a method that optimize the selection of BLDC motor

using an ideal value of propeller efficiency. However, the propulsive efficiency is not proportional to the propeller efficiency and thus, ideal propeller efficiency does not mean that the propulsive efficiency is also ideal. The method developed by Ragot et al [13] modeled the propeller based on Bernoulli equations and momentum theorem. In momentum theorem the thrust produced is like momentum force behind the propeller. This model however cannot properly estimate the effect of different propeller geometry.

Roberts et al [14] have highlighted that flight condition of any micro air vehicle (MAV) operating at altitude between 100 and 1000 m should be considered as under the influence of atmospheric boundary layer (ABL) turbulence. Roberts et al [14] have also concluded that the force coefficients are significantly altered by the presence of turbulence. Thus the conventional aircraft approach to study is unable to anticipate MAV's true flight condition [14]. Among unexpected results from the experimental work [14] are the increase of lift slope with the increase of turbulence intensity, and the decrease of induced drag with the increase of turbulence intensity. The effects of ABL turbulence however was not considered in the previous conceptual design study [7,15-17].

### **1.3 Aim and Objectives**

The aim of this work was to obtain propulsive efficiency value of best combination of propeller-BLDC motor propulsion system. The best propeller-BLDC motor should require the least possible electrical energy at the determined flight conditions.

The objectives of this work are:

- i) To simulate the aerodynamic characteristic of small UAV under the effect of ABL turbulence.
- ii) To investigate the effect of varied propeller geometry, propeller size, airspeed and different rated power of BLDC motor on the propulsive efficiency.

## **1.4 Scope of Work**

The research scope of this thesis involves:

- i) Conceptually design a small UAV airframe that is compatible with existing small UAVs in the market.
- ii) Simulating the UAV airframe in CFD to estimate initial aerodynamic characteristic using turbulence flow model at variable airspeed.
- iii) Constructing constraint diagram to estimate required thrust at different flight condition, and generate Matlab code based on the Goldstein vortex theory of propellers.

## **1.5 Thesis Organisation**

This thesis consists of five chapters. The content of each chapters are as follows:

- Chapter 1: Introduction which provides historical background of small UAV design, problem statement, and aim and objectives of the project.
- Chapter 2: Literature review which includes discussion on aircraft initial design information from critical research area.
- Chapter 3: Methodology used in performing parametric study. The details of qualitative and quantitative considerations to obtain small UAV configuration layout. The details of CFD simulation to obtain aerodynamic characteristic. The details of Matlab code generation to obtain torque and rotational speed of propeller.
- Chapter 4: Validation of CFD simulation and discussion on the parametric study.
- Chapter 5: Conclusions and recommendations for future work.

# Chapter 2

## Literature Review

In this chapter, a brief review of the previous works related to aircraft design information is presented. Studies pertaining to Computational Fluid Dynamics, electric engine, autonomous subsystem architecture and multidisciplinary optimization are examined. Important notes summarizing this brief review are included in the last section of this chapter. A short overview on ABL turbulence and Goldstein Vortex theory is also included in this chapter.

### 2.1 Introduction

Aircraft design information is the essential information describing an aircraft in the aspect of its task, geometry, aerodynamic characteristic, stability, controllability, performance and its effect to the environment. Whenever there is a need to build a new aircraft, this design information of aircraft that are already in service will always be referred to. This information is the initial design information of the new aircraft to be built. The need to perform a more challenging task than what predecessor aircraft is capable of is very often the primary driving factor toward building a new aircraft. In the old days when human flight was nothing but a mere dream, the characteristics of birds are the initial design information used by aeronautic pioneers [18]. Some regard the human flight phenomenon as part of natural evolution and associated it with Darwin's evolution theory [19] but in fact, the presented information shows only evolution or new invention in aircraft engineering technology and not human having any biological wing. New inventions also contribute to initial design information. Invention of components like lifting devices [20] and flow control technology [21], for example, would offer better aerodynamic characteristic.

Design and invention are two different words yet always connected in aeronautic discipline. Allen and Self [22] reviewed a universal concept of creative engineering design by taking

example from various fields of engineering projects and apply the concept to aircraft design project. In particular, to aircraft design, Allen and Self [22] described design as a systematically planned project to achieve or to develop something. While an invention is an unexpected positive result that starts a new design process with engineering aspects are often not understood [22]. UAV design is not very different from aircraft design. In a forecast by Martinez-Val and Perez [23], foreseen that UAVs includingUCAVs (Unmanned Combat Air Vehicles) will be required to perform more dangerous tasks without putting human lives at risk, but it will not completely replace the manned aircraft especially in general aviation and airliners. This means that most knowledge and technology developed in a manned aircraft design project is also applicable in a UAV design project while some technology developed in a UAV design project may not be applicable to manned aircraft design.

Despite inventions of new components, there is a trend of dominant aircraft configuration layout. This trend viewed by Young [24] as a specific phase of industrial innovation where product substitutes will only have improved quality, productivity and process. Young [24] has explored innovation in aviation by examining factors that both promote and inhibit innovation. Sometimes an innovation could lead to an immature technology and thus bearing some risk. Young [24] also examined on how to manage risks of immature technology. According to Young [24], specific phase of industrial innovation is the phase where innovation and invention in several different disciplines are triggered when innovation in a single discipline improves product by only a little [24]. Quadrotor, tilt-rotor and hybrid lift airship [5,25-27] are several new design concepts in aircraft design; success of these concepts will be an invention. These new design concepts offer a possibility of performing a task which available dominant design could not perform.

However, the availability of UAV initial conceptual design information and how to quickly enrich the initial conceptual design information are not studied in previous literature [22-24]. In initial conceptual design information, the vast aspects describing an aircraft are simplified

into several parameters. Important parameters during aircraft conceptual designs are usually the ratio of empty weight to total weight, wing loading, power loading, maximum lift coefficient and drag polar. Without proper organization of initial design information, a new aircraft design project would consume a lot of time. This review will investigate technological advance or invention in different aspect of UAV and how they affect important conceptual design parameters. Computational Fluid Dynamics (CFD), electrical engine and autonomous system architecture and multidisciplinary optimization (MDO) will be the focus of this review.

## **2.2 Computational Fluid Dynamics (CFD)**

CFD is a powerful tool for UAV conceptual design process. European high-lift program [28], for example, has used CFD to speed up optimization process of take-off performance, which closely related maximum lift coefficient. Turbulence, wing-tip vortex and effects of low Reynolds number [29-35] are now research areas that have been receiving much attention. Turbulence and low Reynolds effects are closely related to UAV conceptual design, especially the maximum lift coefficient and drag polar. Wing-tip vortex is related to the airport traffic problem. Even before that CFD has been used to study flow field around high speed X-31 experimental aircraft and has been validated in wind tunnel test. The consequences of the study are still available until today [36-40]. With the ever increasing computing power of computer, CFD is without doubt an essential tool for speeding up the estimation of aerodynamic parameters of new UAV conceptual design.

## **2.3 Electric Engine**

Concurrent with environmental impact is the usage of an electric propulsion system in UAV, which is the permanent magnet brushless DC motor (PMBDCM) [41-43] combined with a propeller. This type of propulsion has a different working principle compared to reciprocating engine and gas turbine engine. PMBDCM uses electrical energy to provide torque to the propeller [13]. Besides its high torque to weight ratio property, PMBDCM

would not lose fuel weight during flight instead it will reduce the energy that can be measured through parameter battery capacity [44-45]. Brinson et al [46] has carried out offline fuel cell powertrain system simulation. The load on the powertrain system [46] was a fixed-pitch propeller attached to an induction motor. The intended power output of the powertrain system [46] was 119 kW with solid oxide fuel cell stack as its primary fuel source. The gap between power flowing out of fuel cell stack and power on induction motor was observed during simulation. The simulation [46] results show that some amount of electrical energy needed to start rotating the propeller and power overshoot is also observed while switching output power level.

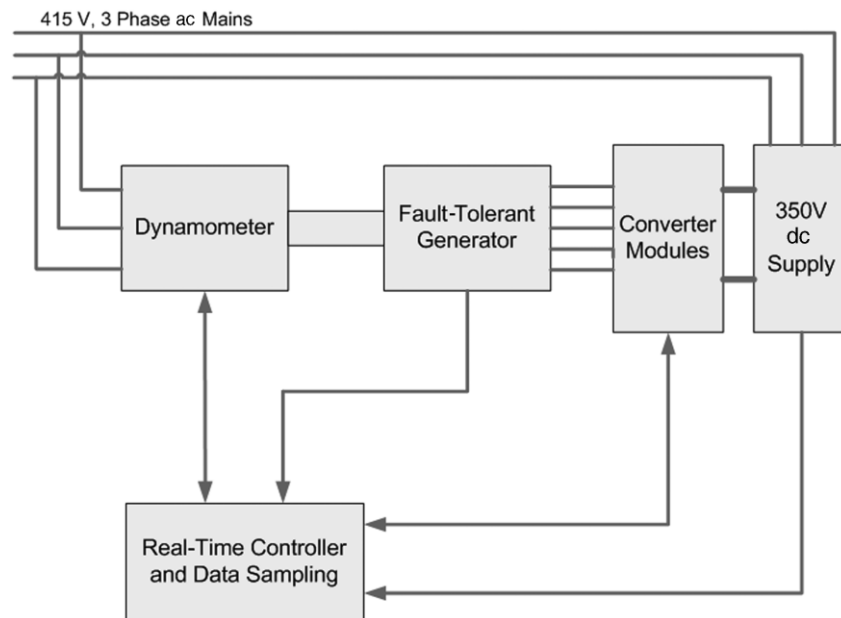


Fig. 2.1 Schematic of testing rig for fault-tolerant 250 kW Permanent Magnet (PM) power generation system [47]

Maybe it is too ambitious to say that electric engine would also replace combustion based engines in all types of aircraft; either manned or unmanned, but such possibility should not be denied when there is a research to develop an electric engine with massive power such as work by Sun et al [47]. In Fig. 2.1, with the suggested 350 V DC supply, one can imagine the massive power of the electric engine [47]. The problem that remains then is to build an energy source with high energy to weight ratio. The ability of a fuel cell to be charged and

discharged during the whole flight mission is therefore, the added advantage aspect of a fuel cell. Bradley et al [48] has studied an energy management strategy for fuel cell powered hybrid-electric aircraft. The fuel cell considered in the study [48] used electrical energy resulting from chemical reaction between hydrogen stored in a tank onboard with oxygen in the atmosphere. At a certain flight condition where fuel cell produces more electrical energy than demanded by electric motor the power management system will store the excessive energy by charging a lithium polymer battery pack. While at other flight conditions where fuel cell could not deliver enough electrical energy, the power management system would discharge the lithium polymer battery pack and add up electrical energy.

For a long-term maintenance consideration, problem of fuel degradation [49] should always be considered. In UAV design [50-52] the efficiency of an electric engine depends on the efficiency of the electronic speed controller (ESC) [53,54]. It is possible that the massive power electric engine pursued by Sun et al [47] would also need a speed controller to regulate the current for different power at different flight conditions. Usage of PMBDCM or simply brushless DC (BLDC) motor has a great effect in UAV conceptual design parameters, especially in estimation of empty weight to total weight ratio, estimation of fuel weight and propulsive efficiency.

#### **2.4 Autonomous Subsystem Architecture**

Autonomous subsystem is principally to substitute human pilot. Thus, the issue of stability and control faced by human pilot since Wright Flyer [55,56] would also need to be tackled by autonomous subsystem. Philips et al [57] described the lacking of data on dynamic stability requirements for UAV as a problematic, hence designer does not know whether the UAV has been designed with a good handling quality or not. Therefore, he established a method that can be applied to any UAV in service, in order to characterize the longitudinal flying qualities of UAV. It is a stepping stone to the evaluation of candidate metrics for establishing flying-quality constraints for UAV.

Duquette [58] then emphasized the importance of simulation before tackling any real-life issue. He added that in traditional method, motions of aircraft are modeled as rigid-body acceleration due to all aerodynamic forces and moments acting on aircraft. Without sufficient data the traditional method is unnecessarily complicated [58]. Therefore, a kinetic-based simulation was proposed. Kinetic-based simulation does not need aerodynamic, propulsive, and gravitational forces to be computed but depend solely on known operating conditions. However, it is uncertain whether kinetic-based simulation alone is enough to develop artificial UAV control system.

Unlike general aviation aircraft [59] flight data collection of UAV is hardly available. However, it is possible to predict an aircraft control and stability characteristic based on its geometry using a computer program. An earlier example of such a computer program was done by Sheldon and Rasmussen [60]. For a given control input, the QFT Flight Control System [60] predicted aircraft attitude, speed and handling quality. However, such computer program may have not yet proven to be accurate and thus the thrust, attitude, speed and handling quality are measured independently. Speed is highly dependent on the relation between aircraft aerodynamic characteristics and thrust. Normally thrust is modeled based on experimental data at different speed [61,62]. For highly maneuverable and high speed aircraft, thrust vectoring control is used and aerodynamic side effects of thrust vectoring is being studied [63,64]. Inertial navigation system (INS) and global positioning system can be used to measure aircraft attitude [65]. Handling quality depends on the aerodynamic derivatives of aircraft configuration [66-68] and even a slight modification to aircraft configuration would change its handling quality [67].

Apart from aircraft attitude, speed and handling quality the trajectory and waypoint simulation and power system simulation [69-71] are also important in the development of autonomous subsystem. Autonomous subsystem often considered successful only if its flight

test is successful [72-75]. It is important to make sure that the UAV correctly and accurately follow the assigned waypoint. However, in UAV conceptual design stage, just like in aircraft design the accuracy of autonomous subsystem is never a considered parameter. More importantly about the autonomous subsystem are its weight and size. Weight of autonomous subsystem would affect the ratio of empty weight to total weight while its size would affect fuselage size and hence, the drag polar.

## **2.5 Multidisciplinary Optimization (MDO)**

Sobieszczanski- Sobieski and Haftka [76] divided MDO into three categories of approaches:

- 1) In the first category, in which two or three disciplines typically interact, a single analyst can acquire the required expertise. This method is MDO for which design variables in several disciplines must be manipulated simultaneously to ensure an efficient design. Example is work by Young [77] to develop a theoretical methodology to investigate the impact on fuel burn during cruise condition for both jet and piston-propeller aircraft, arising from design changes that simultaneously alter the three governing performance parameters of an aircraft in cruise: weight, drag and specific fuel consumption. Other examples are optimization of propulsion system by Ghenaiet [78] and Ghenaiet et al [79]. In both work [78,79], Kreisselmeier–Steinhauser envelope function formulation, associated with a deterministic optimization algorithm was used.
- 2) The second category includes MDO work that is carried out at the conceptual level by using simple analysis tools. Simplicity of the analysis tools enables integration of various disciplinary analyses into a single, usually modular computer program. For example, TAS (Tohoku University Aerodynamic Simulation) code was used to analyze the aerodynamic characteristics, and an in-house solver of conventional real-coded GA was used to optimize the aerodynamic shape of a short-range quiet passenger aircraft [80]. More sophisticated names like HAPMOEAs [81], PrADO [82], and PASS [83] are just another example of computer programs for MDO. In

this category, although an analysis tool is said to be simple, but it is not simple enough for a hand calculation. Aircraft designer would have to rely on the computing power of computer.

- 3) The third category comprises developments that directly address the organizational and computational challenges. Aircraft conceptual design does not fall in this category. This is a level where design is already moving toward detailed design. The aircraft is prepared to be manufactured, flight-tested or even certified. Analyst from different disciplines would need to involve in a discussion. For a small organization, this should not be a too big problem. But for a project which analysts are geographically separate, a Web-based modeling and simulation by Reed et al [84] may be of good help. The potential of Web-based modeling to improve aircraft design process at a multi-national level is due to the ability of the Web to support collaborative modeling and distributed model execution in a heterogeneous computing environment.

To quickly optimize the important parameters at conceptual design stage, use of MDO of second category is helpful.

## **2.6 An Overview on ABL Turbulence and Goldstein Vortex Theory**

Other than the experimental work by Robert et al [14], ABL turbulence is also reported as affecting the drag on a transport aircraft [85]. According to the flight data records analyzed by Brown [85], the ABL turbulence contributes to the decrement of  $-0.8\%$  in First, Second, Third and Final Segment single-engine climb or acceleration performance. The decrement of performance is perhaps caused by a rise in the drag sensitivity to vertical gusts [85]. ABL turbulence is not an easily predicted phenomenon. This is due to the fact that ABL turbulence occurs at different wind speed and turbulent intensity on daily basis [86]. Even a slight variation in operating altitude can also cause a difference in turbulent intensity [87].

The Goldstein vortex theory was proposed as early as 1929 [88]. This theory was developed on the same assumption as airfoil theory [88]. The effective angle of attack on propeller blade is caused by circulation flow that vanishes at the tip of propeller blade [88]. However, this theory is rarely used by researchers due to its complexity and difficult to determine accurately [89]. With the help of computer computing power, compared to other model like Bernoulli equation and momentum theorem [13], it is believed that this theory is more capable in determining the effect of different propeller geometry. Other than in the current work, the attempt to model a propeller by using computer code of Goldstein vortex theory is also reported in the thesis dissertation by Kelly [90].

## **2.7 Summary**

The availability of UAV initial conceptual design information has been reviewed in this chapter. With the ever increasing computing power of computer, CFD is an essential tool for speeding up the estimation of aerodynamic parameters of new UAV conceptual design. There is a possibility that electric engine would replace combustion based engines, but the main problem is to build an energy source with high energy to weight ratio. Apart from accuracy, for small UAV application especially, autonomous subsystem should also be lightweight and in small size. To quicken the optimization process of important parameters at the conceptual design stage, it is important to have simple analysis tools that can be integrated in a single modular computer.

# Chapter 3

## Methodology

In this chapter, the procedure to design the small UAV from scratch is discussed. The development of 3D computational domain and 3D mesh around small UAV is presented and discussed. The simulation tool used in the current project is commercial CFD package, FLUENT 6.3<sup>TM</sup>. The governing equation of Goldstein vortex theory of propellers is explained, and the Matlab code of the equation is presented.

### 3.1 Initial Aerodynamic Characteristic of Small UAV

The initial aerodynamic characteristic was obtained through the aircraft conceptual design procedure. The first three steps of overall conceptual design procedure are first estimation of weight, optimizing critical performance parameter and determination of configuration layout. Design of the small UAV was constrained mainly by a set of five design requirements. These design requirements are based on the typical performance data of hand-launch UAV available in the market [91] as in Table3.1:

- i) 0.2 kg payload; small surveillance camera
- ii) Stall speed of 36 km/h
- iii) Design cruise speed of 55 km/h at altitude 100m
- iv) Climb to cruise altitude in 30 seconds
- v) Maximum cruise speed of 72 km/h

Table3.1 Performance data of UAV in the market [91]

UAV Name	Weight, kg	Maximum Speed, km/h	Maximum altitude, m
Dragon Eye	2.6	80	300
Pointer FQM-151	3.6	88	3750
PUMA	5.0	96	3750
Evolution	2.9	72	300

### 3.1.1 Weight Buildup

According to Raymer [8], for non-military manned aircraft the total weight of the aircraft as it begins its mission should consist of crew weight, payload weight, fuel weight and empty weight, which expressed mathematically in Eq. 1.

$$W = W_{crew} + W_{payload} + W_{fuel} + W_{empty} \quad (1)$$

In the case of small UAV, the crew weight in Eq. 1 is absent. But weight of autonomous and navigation subsystems were taken into account together with payload weight. Small UAV in this work was intended to use Li-Po battery as the fuel source. Compared to Ni-Cd battery, Li-Po battery has a higher energy to weight ratio. In Raymer [8], first estimation of the fuel fraction is based upon mission flight profile, aerodynamics of the aircraft and fuel consumption. In later part of this thesis, it will be shown that for a small UAV using battery as fuel, electrical charge consumption or current consumption, which directly related to battery capacity is a parameter that should replace fuel consumption.

Table 3.2 Sums of  $W_{auto-sub}$ ,  $W_{payload}$  and  $W_{battery}$

Weight Class	Subclass	Example(s)	Estimated Weight, kg
Payload	-	-	0.20
Autonomous subsystems[16]	Sensors	Baro-altimeter, Differential Pressure sensor, GPS receiver, Infrared inclinometer	1.24
	Communication hub	Microcontroller	
	Processor	Personal Digital Assistant, etc.	
Li-Po battery	Reserved components	Ni-Cd battery for camera	0.21
	-	Thunder Power 2700 mAh 11.1V	

Just like fuel the more current consumed the more battery capacity needed and the heavier battery weight. Unlike fuel, which amount can be customized as a continuous function, battery capacity currently available in the market as pre-customized selection or as a discrete

function. Thus, for first estimation, it was more convenient to use weight of battery as a constant number rather than in a fraction form. The sums of autonomous subsystem weight, payload weight and battery weight are in Table 3.2.

Like manned aircraft, the empty weight of small UAV was estimated statistically from historical trends. Empty weight includes structural weight, fixed equipment weight and weight of the propulsion system. Through data collected and tested by Hung et al [15] it can be said that log of small UAV empty weight grows linearly with log of small UAV total weight. The constant A, and B in Eq. 2 used the same value accepted by Hung et al [15]. Eq.3 is the fraction form of Eq. 2. By inserting Eq. 3 in Eq. 1, and solving it numerically as in Eq. 4, gave the initial estimation of small UAV total weight.

$$\log_{10} W = A + B \log_{10} W_{empty} \quad (2)$$

$$\frac{W_{empty}}{W} = 10^{\frac{-A}{B}} W^{\left(\frac{1}{B}-1\right)} \quad (3)$$

$$W - 10^{\frac{-A}{B}} (f_{lb-kg} W)^{\frac{1}{B}} = W_{auto-sub} + W_{payload} + W_{battery} \quad (4)$$

### 3.1.2 Critical Performance Parameters

The first critical parameter was the maximum lift coefficient that led to airfoil selection and wing sizing. The small UAV was intended as a hand-launch and thus take-off and landing profile were not considered. The small UAV also would not use high-lift devices. Thus, the airfoil selected should be able to provide maximum lift on the wing at cruise stall speed condition as high as possible. Stall speed is the slowest speed the small UAV can fly before it starts losing lift. Since the small UAV in this work is intended to fly at a low cruise speed,

it is important to ensure that there is some margin between the normal cruise speed and the stall speed.

For conventional manned aircraft, Raymer [8] suggested that a good estimation of 3D wing maximum lift coefficient should be about ninety percent of 2D airfoil. However, to allow some margin between normal cruise speed and stall speed it was estimated that 3D wing maximum lift coefficient would be eighty percent of 2D airfoil as in Eq. 5. The sizing of wing area due to stall speed requirement is presented by Eq. 6. The wing airfoil was selected based on the low Re number 2D airfoil data provided by Eppler [92].

$$C_{Lmax} = 0.8c_{lmax} \quad (5)$$

$$\frac{W}{S} = \frac{1}{2}\rho_{100m}U_{stall}^2C_{Lmax} \quad (6)$$

The other critical parameters at conceptual design stage are wing loading, lift to drag ratio and power loading. The wing loading was already frozen in wing sizing. Lift to drag ratio and power loading were determined later after initial configuration layout was available and CFD analysis was done.

The wing loading is the weight of the small UAV divided by the wing's reference area. Wing loading affects stall speed, climb rate, takeoff and landing distances, and turn performance [8]. Based on the estimation of total weight, higher wing loading results in a smaller size of wing. In this work, a small wing is preferred in order to reduce drag. Lift to drag ratio is a measure of the small UAV design's overall aerodynamic efficiency. This parameter is highly dependent upon the configuration arrangement. In level flight the lift must be equal to the weight of the small UAV. Thus, lift to drag ratio is solely dependent upon drag [8]. In this

work, the drag of the small UAV configuration was estimated by considering the effect of ABL turbulence.

Power loading is a parameter associated with propeller-powered aircraft. This parameter is expressed as the weight of the small UAV divided by the rated power of the engine. Power loading directly affects the performance of the small UAV. A small UAV with a higher power loading will accelerate more quickly, climb more rapidly, reach a higher maximum speed, and sustain higher turn rates [8].

### **3.1.3 Configuration Layout of Small UAV**

The configuration layout of the small UAV was obtained following Roskam's [10] methodology with the aid of Advanced Aircraft Analysis (AAA) software. AAA is the industry standard aircraft design, stability, and control analysis software developed by DARCorporation. This software was used to handle design parameters so that all the parameters can be accessed at any time. Conceptual design of small UAV involves thousands of unique parameters and hundreds of mathematical models. If calculations were to use spreadsheets, the design process would consume a lot of time. However, the aerodynamic module of this software is a semi-empirical method and based on the aerodynamic data of subsonic manned aircraft. Therefore, this software was used only to assess the static stability characteristic of small UAV at first design iteration.

Summarizing the methodology [10], the procedure to create the configuration layout of small UAV consists of qualitative and quantitative considerations. The wing planform, fuselage configuration, propulsion system with either pusher or tractor propeller, and empennage configuration layout, are the qualitative aspects of small UAV configuration layout. The design constraints of these aspects cannot be modeled mathematically. The size of wing area is constrained mainly by stall speed requirement. The arrangement of wing, fuselage, and

size and position of the empennage are constrained by the static stability requirement. Any design parameter affected or affecting the static stability requirement is considered as quantitative.

Sizing of empennage and control surfaces followed volume method, and estimation was based on homebuilt aircraft data in Roskam [10]. The criterion for taking homebuilt aircraft as reference over other types of aircraft was in case the small UAV need to be flown in RPV mode, it should have adequate stability and yet easy to handle even by trainee pilot. Homebuilt aircraft generally satisfied this criterion. The arrangement and disposition of wing, fuselage, and empennage were finalized through iterative design trials in AAA. The iteration continued until both longitudinal and lateral directional static stability requirement were satisfied.

For inherent longitudinal static stability, the zero lift pitching moment coefficient should be positive and pitching moment derivative due to angle of attack should be negative with adequate static margin (SM) as in Eq. 7 and Eq. 8 respectively. Roskam [10] suggested that initial estimate of SM should be about ten percent but data provided by Raymer [8] have shown that SM of final design could be less than ten as long as the aircraft is trimmable. Furthermore, the speed range of small UAV designed can be considered as small. For inherent directional static stability, the minimum yawing moment derivative due to sideslip force should follow Eq. 9.

$$C_{m0} > 0 \quad (7)$$

$$C_{m\alpha} < 0 \quad (8)$$

$$C_{n\beta} \sim 0.0573 \text{ rad}^{-1} \quad (9)$$

At the end of the configuration layout design stage UAV lift coefficient and drag polar were calculated by AAA software but results were insignificant to determine the power loading since ABL turbulence effect was not accounted.

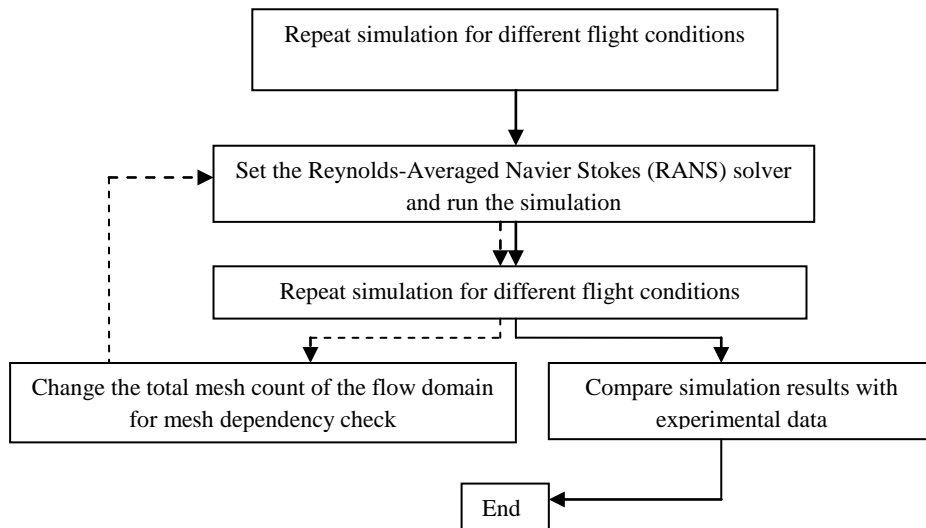


Fig. 3.1 The flow chart of CFD simulation procedure

### 3.2 Computational Fluid Dynamics (CFD) Analyses

To obtain a more correct anticipation of flow-field around small UAV [8], lift coefficient and drag polar was obtained via CFD simulation. The procedure of running the CFD simulation is as shown in flow chart in Fig. 3.1.

For CFD simulation, in order to reduce computational time, only symmetrical half of the UAV model was generated. Distance from the fuselage nose to flow domain front end was 1.2 m and the distance from the fuselage aft to flow domain trailing end was about 2 m. Distance from wing tip to flow domain far side was 1.32 m. The distance from wing top surface to flow domain top end, and from the fuselage bottom surface to flow domain bottom end were 0.824 m and 0.94 m respectively. To control the number of mesh count in the flow domain, the flow domain was divided into two flow region as in Fig. 3.2.

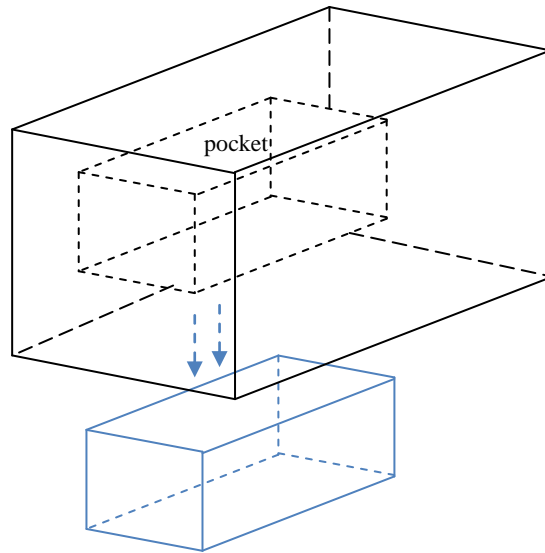


Fig. 3.2 The flow domain divided into main and smaller region.

The main flow domain volume is a brick while the smaller region of the flow domain is like a pocket subtracted from the main flow domain. The two flow domain regions attached with each other at five faces. The mesh type and mesh size on those faces are identical. The boundary conditions of the faces on smaller region are identical to the outer faces on main flow domain. The boundary condition of the inner faces on main flow domain attached to smaller region was set to velocity inlet. The main flow domain velocity inlet faces and pressure outlet face are shown Fig 3.3.

The coarse tetrahedral mesh was developed in the main flow domain region with mesh interval size ranging from 0.05 m to 0.25 m. Smaller mesh closer to small UAV surface was developed in the smaller region. The range of mesh interval size was 0.0025 m to 0.005 m on small UAV surface and 0.05 m on farther end. Mesh near small UAV surface was then refined using conformal volume adaption technique with a minimum cell volume of  $1.4 \times 10^{-8} \text{ m}^3$ . The total mesh count in the computational domain was 823583. Fig. 3.3 shows the computational domain with the given boundary conditions. The dimension of the small UAV can be viewed in Fig. 4.1.

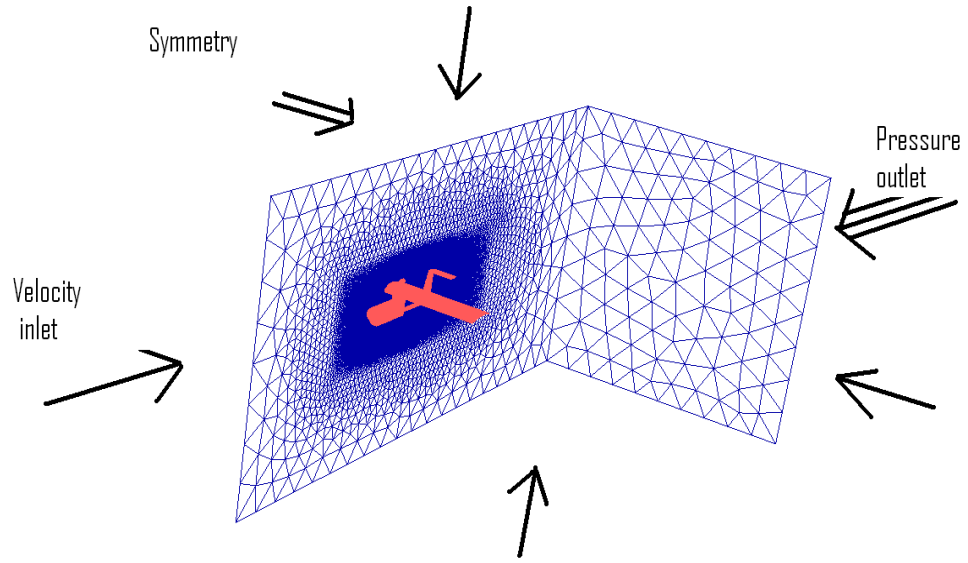


Fig. 3.3 Small UAV computational domain

The numerical simulation was carried out in Fluent 6.3 for a Mach number of 0.045 using the shear-stress transport (k- $\omega$  SST) turbulence model. The integral form of the transport equation for a general scalar,  $\phi$ , on an arbitrary control volume,  $\bar{V}$ , which implemented in Fluent 6.3<sup>TM</sup> [93] is as shown below:-

$$\frac{d}{dt} \int_{\bar{V}} \rho \phi (\bar{u} - \bar{u}_g) d\bar{A} = \int_{\partial \bar{V}} \Gamma \Delta \phi \cdot d\bar{A} + \int_{\bar{V}} \bar{S}_\phi d\bar{V} \quad (10)$$

To avoid confusion the symbol for control volume used  $\bar{V}$  instead of  $V$  and  $\bar{S}$  instead of  $S$ . Justification for SST k- $\omega$  turbulence model accuracy and reliability are based upon the study by Rumsey and Spalart [29], which indicates that SST k- $\omega$  is a good turbulence model since it also helps reducing grid dependence of the transitional behavior and thus saving simulation time. This was also confirmed through comparison between two-dimensional analysis and experimental data by Ahmad et al [93]. While comparison with experimental results by Jammalamadaka and Nagib [30] concluded that this turbulence model is a good choice for

the prediction of the skin-friction. Wingtip vortex is not of the interest of this paper and whatever conclusion made by Churchfield and Blaisdell [31] thought to be insignificant.

The first simulation was run at cruise speed at angle of attack [-3, -2, -0.5, 1, 2, 5, 6, 9, 10, 13, 14, 15, 16, 17] degrees. Simulation was re-run at maximum cruise speed and stall speed for different Re number at angle of attacks [-0.5, 5, 13, 17]. Mesh dependency check was performed with three different flow domain total mesh count; 283096, 438594 and 823771. Minimum cell volume settings for volume adaptation were  $1.8 \times 10^{-7} \text{m}^3$ ,  $5 \times 10^{-8} \text{m}^3$  and  $1.4 \times 10^{-8} \text{m}^3$  respectively with  $y^+$  was set to 1. Simulation for mesh dependency check was run at cruise speed at angle of attacks [-3 1 6 14].

### 3.3 Preliminary Performance Analyses

The maximum speed requirement of the small UAV was as described by Eq.11, and the time to climb requirement was the inverse of Eq.12. The power to weight ratio (P/W) is related to time to climb requirement by Eq.13 and Eq.14. The  $C_L^{3/2}/C_D$  ratio in Eq.12 was set to be near maximum and determined graphically from CFD cruise drag polar. Power to weight ratio in Eq.12 is normally multiplied with a propulsive efficiency value. However, for the purpose of the current work, the efficiency was set to 1 as it is the pure desired mechanical power on the propeller. Based on UAV model of Iscold et al [17], the absolute altitude  $h_{\text{abs}}$  was assumed to be 150 m.

$$\frac{W}{P} = \frac{2(W/S)}{\rho U^3 C_D} \quad (11)$$

$$\frac{P}{W} = RCP + \sqrt{\frac{2(W/S)}{\rho}} \frac{1}{C_L^{3/2}/C_D} \quad (12)$$

$$RCP = RC_o \left(1 - \frac{h}{h_{abs}}\right) \quad (13)$$

$$RC_o = \left(\frac{h_{abs}}{t_{cl}}\right) \ln \left(1 - \frac{h}{h_{abs}}\right)^{-1} \quad (14)$$

### 3.4 Parametric Study of Propulsive Efficiency

#### 3.4.1 BLDC Motor Characteristic

Normally power (P) in any flight condition is measured mechanically as a product of thrust (T) of the propulsion system and airspeed (U) of aircraft as in Eq.15. While in electronic and electrical system, power is often a product of current (I) and voltage (V) as in Eq.16. Thus, the propulsive efficiency,  $\eta$  in the current work is measured as the mechanical power on propeller divided by the electrical power across the BLDC motor as in Eq. 17.

$$P = TU \quad (15)$$

$$P = IV \quad (16)$$

$$\eta = \frac{TU}{IV} \quad (17)$$

With analogy to reciprocating engine's specific fuel consumption (SFC), BLDC motor's  $K_t$  constant with a unit of A/Nm is the parameter that indicates the amount of Ampere (A) current drawn from the battery for 1 Nm torque produced by the engine [94]. The life of the battery is characterized by battery capacity which is described as ampere-hour (Ah) [48]. The current drawn by BLDC motor is mainly to provide enough torque to overcome the aerodynamic resistance experienced by the propeller [13]. The aerodynamic resistance on the propeller depends on the size and geometrical shape of the propeller blade itself. The other constant that characterizes BLDC motor is the back EMF constant  $K_v$  having unit V/rads<sup>-1</sup>. The rotational speed in BLDC motor generates back EMF which will be opposed by the

voltage from battery [94,95], and the back EMF being directly related to propeller advance ratio.

BLDC motors in the market are produced by several manufacturers like Scorpion, Hacker, Himax and Hyperion. Among these manufacturers, only Himax provides the information of ESC rated current. The other manufacturers provide only the maximum current of BLDC motor. The information of ESC rated current is an initial indicator of current range at which the back EMF constant holds true. Further discussion of rated current is in Chapter 4.

Therefore, four Himax BLDC motor candidates were selected for parametric study, and their technical specifications are as in Table 3.3. Each BLDC motor is connected to its own suitable electronic speed controller (ESC) and a series consisting of three Li-Po batteries, which results in a maximum voltage of 11.1 V. Even though each BLDC motor is connected to maximum 11.1 V voltage source, it was estimated that maximum effective voltage each BLDC motor uses to convert into propeller rotational speed is only 10 V. The loss due to motor resistance is therefore included in estimating the maximum voltage from the Eq. 18. Ten percent reserve current should be accounted for accelerating propeller to the desired rotational speed [94]. Maximum effective rotational speed  $\omega_{max}$  and 90 percent of maximum ESC current rating multiplied with torque constant  $K_t$  gives the BLDC motor constraints.

$$\omega_{max} = K_v(V - 2R_m I) \quad (18)$$

Table 3.3 BLDC motor candidates

Motor Himax	Rated power (W)	$K_v$ rpm/V $\times 10^3$	$K_t$ Nm/A $\times 10^{-2}$	ESC rating (A)	Weight (kg)	Motor resistance, $R_m$ ( $\Omega$ )
HC3516-1130	350	1.13	0.845	10-34	0.134	0.03
HC3522-0700	400	0.7	1.364	8-29	0.162	0.049
HA3630-1000	600	1.0	0.955	15-30	0.230	0.05
HA2825-2700	400	2.7	0.354	8-30	0.138	0.041